Hybrid Fuzzy-PI Control of DFIG Power Associated with a Variable Speed Wind Energy Conversion System

Hedayat Akhbari[1], Javad MashayekhiFard[2*]

Abstract–The rotor side converter (RSC) controls active and receptive powers at the stator side of DFIG. The turbine current in axis d (id) is modeled utilizing the parameters of a 660 kW wind turbine. The appraised wind speed within the specified wind turbine is 15 (m/s) and the wind cut-in and cut-out speed is 4 (m/s) and 25 (m/s) individually. In this paper, we utilized tuning the hybrid fuzzy PI controller based on the Mamdani inference system and selecting the triangular membership functions, and compare with three strategies. The proposed strategy is way better than a conventional PID controller, fuzzy logic, and hybrid fuzzy-PI controllers with Gaussian membership functions for active and reactive power control. Simulation and comparison think about are utilized to appear the effectiveness of the proposed hybrid fuzzy-PI controllers with triangular membership functions and fewer errors, ripple, and overshoot have been gotten.

1. Introduction

Due to the significant advantages of wind power plants such as producing less level of CO_2 and less environmental negative impacts, in comparison with thermal power plants, the power output from wind energy tremendously increased in the last decade. According to the Global Wind Energy Council (GWEC) annual report Fig.1, the worldwide wind power installation has reached 539 GW by the end of 2020 [1]. Likewise, wind power installation in the Islamic Republic of Iran has rapidly increased from 94 MW in the March of 2012 and reached 110 and 194 MW by the same month in 2014 and 2018 respectively [2][3][4]. Among different types of generators used in wind energy conversion systems (WECS), the variable-speed WECSs based on doubly fed induction generators (DFIG), owing to their advantages of better performance over a wide range of wind speed, the capability to operate under and above synchronous speed, control of active and reactive power of stator simultaneously and compatibility with grid static and dynamic status, have been found superior [5]. According to multiple low-speed designs of DFIGs, gearboxes are required. Three-stage (3S) gearboxes have been commercially released to enhance the feasibility of DFIGs. In spite of the problems associated with a 3S gearbox, the DFIG still has superiority over other types of generators like direct drive synchronous generators (SG) and direct drive permanent magnet generators (PMG). The results of comparison based on a 3S-DFIG with two other types of generator used in WECSs have been shown in Table I. It can be concluded that the total weight of direct drive PMG is approximately 4.5 times higher than similar DFIG. The stator diameter of a DFIG is one-sixth of a direct drive PMG [6]. Two implemented back-to-back converters, called rotor side converters (RSC) and grid side converters (GSC), are used in a DFIG. Fundamentally, RSC synchronizes the phase, frequency, and amplitude of the stator vector with the grid vector, which are prerequisites of grid connection. In addition, it controls the active and reactive power generation of a DFIG. On the other side, the DC-link voltage and the exchanging reactive power between the generator and the grid are controlled by GSC. In a DFIG, the size of converters has been reduced to 25% up to 30% of generator capacity [7-9].

1 Department of Electrical Engineering, Sabzevar Branch, Islamic Azad University, Sabzevar, Iran.Email:hedayat.akhbari@gmail.com

2* Corresponding Author :Department of Electrical Engineering, Sabzevar Branch, Islamic Azad University, Sabzevar, Iran. Email: mashayekhi@iaus.ac.ir
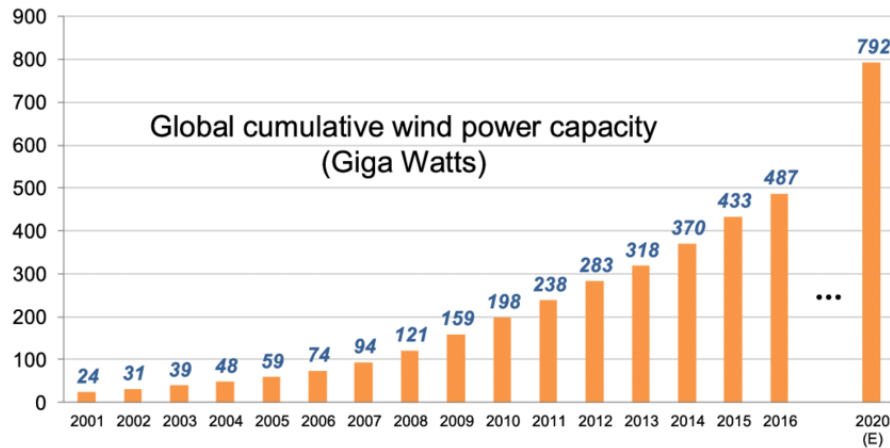
Fig. 1 Global installed wind capacity 2001-2017

TABLE I.   COMPARISON OF WIND TURBINE GENERATORS [6]

Index	Wind turbine generators		
	3-Stage geared DFIG (%)	Direct drive synchronous (%)	Direct permanent magnet (%)
Weight	100	≈850	≈450
Stator radious	100	≈600	≈600
Estimate of total cost	100	120	≈105
Power losses	100	95	≈65

In a grid-connected DFIG, the stator is directly connected to the grid, and due to the limited power rating of its excitation; the generator operation is completely affected by grid disturbance. Hence, in order to obtain maximum efficiency under different statuses of wind and grid load profiles, the control structure of a DFIG should be considered carefully [5-9]. Fuzzy logic controllers according to their intrinsic properties, in comparison with PI controllers, propose self-tuning and robust control of a WTES in transient and high fluctuating characteristics of wind velocity [8]. They have high efficiency in uncertain and non-linear control systems and there is no need for the knowledge of exact models. In [10], the proposed maximum power point controller works capably with wind speed grouping and tracks the power exceptionally well, in reality, in moo wind conditions to the vast wind speed collection. In [11] considering that the control coefficients K_I and K_P interior of the PI controller utilized interior of the space vector change strategy needs to be tuned, three clever approaches, especially particle swarm optimization (PSO), the imperialist competitive algorithm, and teaching–learning based optimization, have been in utilized to this conclusion and a comparison was made between the comes around gotten from the three approaches. In [12], cutting-edge optimization strategies for maximum power point controllers utilizing artificial intelligence like fuzzy control

and neural network control are too shown. In [13], the component of the dc-link stream and how the dc-link stream impacts the small-signal characteristics of the DFIG system are portrayed, to start with. At that point, a pointer work that models the dc-link enthusiastic behavior is first characterized and after that gets based on consonant linearization methodology. In this paper, the first wind turbine modeling consisting of a wind energy background, drive train model, and generator model was presented. After formulating the problem, the control strategies of DFIG with fuzzy controller and hybrid fuzzy-PI controller were displayed. After that, the proposed controller is implemented and compared with 3 other methods for active and reactive control, and finally, conclusions and references were given.

2. Wind Turbine Modelling

2.1 Wind Energy Background

The common association chart of DFIG in grid-connected mode is as appeared in Fig 2. The stator of DFIG is associated with three stage supply through the framework and the rotor is associated with voltage source inverters through a common DC connect. Control within the wind stream agreeing to [14] and [15] can be communicated as:

$$P_{air} = 0.59\rho A V^3 \tag{1}$$

Where P_{air} is airflow power (watts), 0.59 is Betz constant ρ is air density (kg/m^3), A is the swept area by the turbine blades (m^3) and V is the wind speed (m/s). The power output by the wind turbine rotor is:

$$P_m = Cp.P_{air} \ , \ C_p = \frac{P_m}{P_{air}}, TSR(\lambda) = \frac{\omega_r R}{V_w} \ , \ \omega_r = \frac{2\pi n}{60} \tag{2}$$

Where P_m (watt) represents the amount of actual power output by the wind turbine (active output power) over the amount of theoretical available power pair, C_p is the aerodynamic productivity of a wind turbine is portrayed by the coefficient of execution, moreover called the power coefficient, which isn't consistent and depends on two
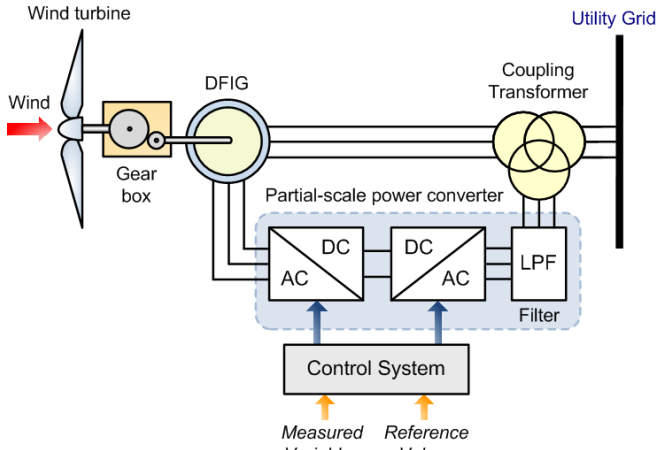
Fig. 2. Wind Power Generation with DFIG[15]

Fig. 3.Cp versus Tip Speed Ratio (λ)

essential parameters specifically: tip speed ratio TSR or λ is characterized to be the ratio of the rotor speed to wind speed, and β (degree) blade pitch angle (the angle at which the blade is turned along longitude axis). ω_r (rad/s) is the mechanical angular velocity of the turbine, R(m) is the radius of turbine blade, V_w (m/s) is the wind speed, and n(rpm) is the rotational speed. The pitch angle (β) and the rotor speed ω_r are two parameters that can be utilized for the control of the turbine. Optimization of the power underneath the nominal power happens at the most extreme value of C_p, which cannot be happened unless choosing β rise to βopt and λ consistent at its ideal esteem λopt. In any case, ω_r can be built up from the streamlined information of the rotor, much less demanding than V_m; subsequently, it is utilized rather than λ in optimization [16]. Based on [16-18]the closest coefficient Cp found as appeared underneath:

$$\lambda_i = \frac{1}{\lambda + 0.02\beta} - \frac{0.002}{\beta^3 + 1} \qquad (3)$$

$$C_p = 0.571\left(\frac{116}{\lambda_i} - 0.4\beta - 5\right)e^{\frac{-21}{\lambda_i}} - 0.0065\lambda_i \qquad (4)$$

By operating a turbine at a variable rotational speed, it is possible to achieve the maximum Cp over a wide range of wind speeds. Although it should be considered that based on the Betz Limit, the maximum of Cp will not exceed 0.593 [14]. A wind energy turbine starts to generate power from the cut-in velocity of wind (4 m/s) and continues to produce power till the cut-out velocity of 25 (m/s). The rated wind speed is usually around 12-14 (m/s) [19]. In Fig.3 Cp versus tip speed ratio (λ) and in Fig.4 Cp for pitch angles β=[0 10 20 30] versus wind velocity (m/s) and the curve of measured data [20] has been represented (βopt=0). Based on (7) In Fig.5 output power of the turbine (p.u.) versus wind velocity(p.u.) and in Fig.6 electrical output power (p.u.) versus wind velocity (m/s) has been represented.
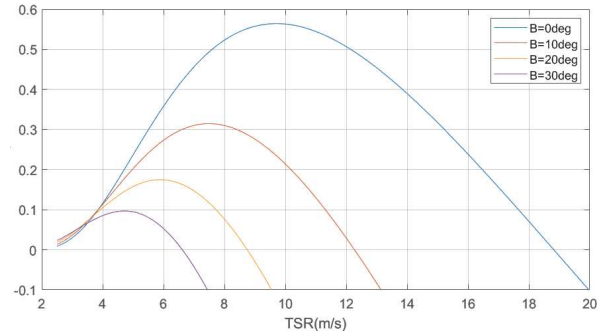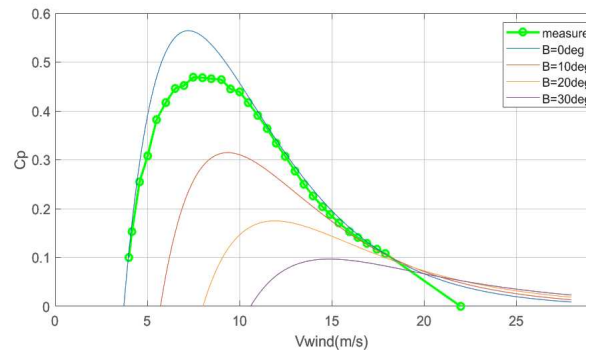
Fig. 4   *Cp* versus *V wind*
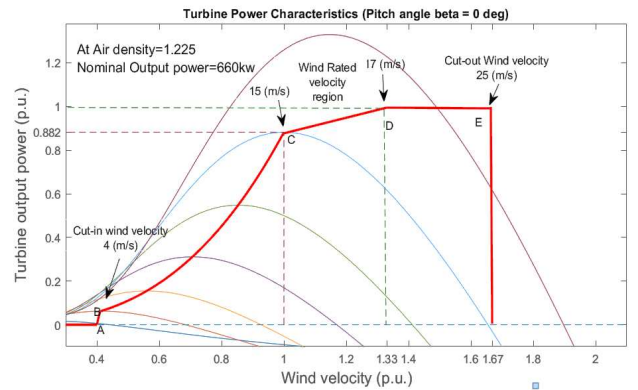
Fig. 5. Turbine output power (p.u.) versus Turbine speed (p.u.) at air density 1.225 (kg/m³)
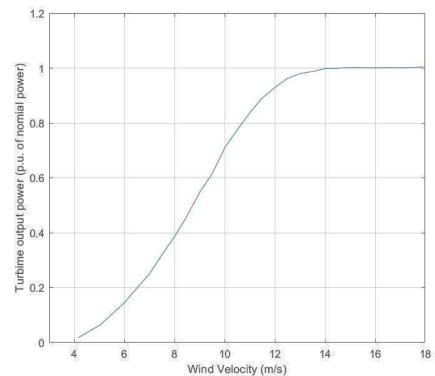
Fig. 6. Electrical output power (p.u.) versus wind velocity(m/s)
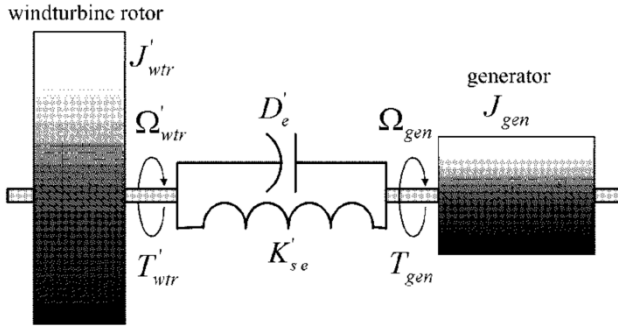
Fig.7. Two Mass Drive Train Model

In order to obtain the output torque of the turbine, the following relationship is employed [21]:

$$T_{m_{(pu)}} = \frac{P_m(pu)}{\omega_r(pu)} \tag{5}$$

2.2 Drive Train Model

In [9] a model of a drive train in which the whole parts of a turbine are modeled as one mass is presented. In the two-mass model of the drive train, the set of turbine and gearbox is considered as one mass; while the rotor and its equipment are taken as a separate mass. Fig. 7 shows the model of two mass drive trains transferred to the generator shaft side. Following relations can be driven [21]:

$$T_t' = J_t' \frac{d\omega_t'}{dt} + D_m'(\omega_t' + \omega_g') + D_t'\omega_t' + k'(\theta_t' + \theta_g) \tag{6}$$

$$-T_g = J_g \frac{d\omega_g}{dt} + D_e'(\omega_g - \omega_t') + D_g'\omega_g + k'(\theta_g - \theta_t') \tag{7}$$

$$\omega_t' = \frac{d\theta_t'}{dt} \ , \ \omega_g = \frac{d\theta_g}{dt}, \ k' = \frac{k_g k_t/n^2}{k_g + k_t/n^2} \tag{8}$$

$$J_t' = \frac{1}{n^2}J_t, \ D_t' = \frac{1}{n^2}D_t \ , \ D_m' = \frac{1}{n^2}D_m \tag{9}$$

Where n signifies gearbox turn proportion, Tt′ wind turbine torque exchanged to the generator shaft-side, Tg generator torque, ωt′ turbine rotor speed exchanged to the generator shaft-side, Jt′ turbine inertia moment exchanged to the generator shaft-side, Jg generator rotor's inertia moment, Dm′ damping proportion of the turbine exchanged to the generator shaft-side, Dt′ damping proportion of turbine exchanged to the generator shaft side, Dg damping proportion of generator shaft, kt spring proportion of generator shaft, kt spring proportion exchanged to the generator shaft-side, kg spring proportion of generator shaft, k′ add up to spring proportion (torsion spring proportion) that's gotten by equaling the spring proportion of the generator shaft and turbine shaft. In these connections, the amounts of low-speed shaft side (turbine shaft) are exchanged to high-speed shaft side (generator shaft) famous by the prime sign " ′ ".

2.3 Generator Model

To control the real power Ps and reactive power Qs at the stator side, the magnitude of DC-link voltage Edc is kept steady. An identical circuit of DFIG in a dq reference outline has appeared in Fig.8. This model show is commonly utilized to extricate DFIG. The supply voltage angle is utilized within the plot; in this manner, the real axis d is adjusted with the same phasor of supply voltage and Vsq=0, at that point the output powers of the framework side converter are given by the taking after expressions [5] [8][9] [22]:
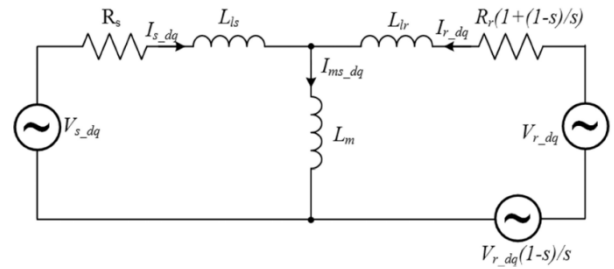
Fig.8   Induction Generator Equivalent Circuit

$V_{ds}, V_{qs}, V_{dr}, V_{qr}$	dq-axis stator and rotor voltage
$\varphi_{ds}, \varphi_{qs}, \varphi_{dr}, \varphi_{qr}$	dq-axis stator and rotor flux
$I_{ds}, I_{qs}, I_{dr}, I_{qr}$	dq-axis stator and rotor current
R_s, R_r	stator and rotor resistance
L_s, L_r	stator and rotor self-inductance
M	self-mutual inductance
p	pole numbers
ω_s, ω_r	stator and rotor rotary field speed
U	grid voltage

$$V_{ds} = R_s I_{ds} + \frac{d}{dt}\varphi_{ds} - \omega_s \varphi_{qs} \tag{10}$$

$$V_{qs} = R_s I_{qs} + \frac{d}{dt}\varphi_{qs} + \omega_s \varphi_{ds} \tag{11}$$

$$V_{dr} = R_r I_{dr} + \frac{d}{dt}\varphi_{dr} - \omega_r \varphi_{qr} \tag{12}$$

$$V_{qr} = R_r I_{qr} + \frac{d}{dt}\varphi_{qr} + \omega_{sr}\varphi_{dr} \tag{13}$$

$$\varphi_{ds} = L_s I_{ds} + M I_{dr} \ , \ \varphi_{qs} = L_s I_{qs} + M I_{qr} \tag{14}$$

$$\varphi_{dr} = L_s I_{dr} + M I_{ds} \ , \ \varphi_{qr} = L_s I_{qr} + M I_{qs} \tag{15}$$

DFIG electromagnetic torque (C_{em}) can be expressed as:

$$C_{em} = \frac{3}{2}(\varphi_{ds} I_{qs} - \varphi_{ds} I_{ds})$$

(Error! Bookmark not defined.)

$$\varphi_{ds} = \varphi_s \ , \ \varphi_{qs} = 0 \tag{16}$$

$$C_e = -p\frac{m}{L_s}\varphi_{ds}I_{qr}, V_{ds} = 0, V_{qs} = V_s = \omega_s\varphi_s \quad \text{(Error!}$$

Bookmark not defined.)

$$I_{ds} = -\frac{M}{L_s}I_{dr} + \frac{\varphi_s}{L_s} \ , \ I_{qs} = -\frac{M}{L_s}I_{qr} \tag{17}$$

$$V_{dr} = R_r I_{dr} + \left(L_r - \frac{M^2}{L_s}\right)\frac{dI_{dr}}{dt} - \omega_r \left(L_r - \frac{M^2}{L_s}\right)I_{qr} \qquad (18)$$

$$V_{qr} = R_r I_{dr} + \left(L_r - \frac{M^2}{L_s}\right)\frac{dI_{qr}}{dt} - \omega_r \left(L_r - \frac{M^2}{L_s}\right)I_{dr} + \omega_r \frac{M}{L_s}\varphi_s \quad (19)$$

The stator active and reactive power equations in dq- axis are:

$$P_s = V_s I_{qs} \ , \ Q_s = V_s I_{ds} \qquad (20)$$

$$P_s = -V_s \frac{M}{L_s}I_{qr} \ , \ Q_s = -V_s \frac{M}{L_s}I_{dr} + \frac{V_s^2}{L_s \omega_s} \qquad (21)$$

$$\varphi_{ds} = \varphi_s \ , \ \varphi_{qs} = L_s I_{qs} + M I_{qr} = 0 \qquad (22)$$

$$V_{ds} = R_s I_{ds} + \frac{d}{dt}\varphi_{ds} \ , \ V_{qs} = R_s I_{qs} + \omega_s \varphi_{ds} \qquad (23)$$

The voltage drops are neglected: $\qquad R_s I_{ds} = 0$ and $R_s I_{qs} = 0$so we have:

$$V_{ds} \cong \frac{d}{dt}\varphi_s \ , \ V_{qs} \cong \omega_s \varphi_s \quad (24)$$

The work in a steady state $\varphi_s \cong cte$ so we can write:

$$V_{ds} = 0 \ , \ V_{qs} = \omega_s \varphi_s \qquad (25)$$

The DFIG is connected to the grid, so we have:

$$V_{qs} = U = cte \ , V_{ds} = 0 \qquad (26)$$

$$\varphi_{ds} = \varphi_s = \frac{U}{\omega_s} = \frac{U}{2\pi f} \ , \ \varphi_{qs} = 0 \qquad (27)$$

Now by using equation 15, the equations 11 ,12 become:

$$V_{rd} = R_r I_{dr} + \sigma L_r \frac{dI_{dr}}{dr} - \omega_r \sigma L_r L_{dr} \qquad (28)$$

$$V_{qr} = R_r I_{qr} + \sigma L_r \frac{dI_{qr}}{dt} - \omega_r \left(\frac{M}{L_s}\varphi_s + \sigma L_r L_{dr}\right) \qquad (29)$$

$$\sigma = \left(1 - \frac{M^2}{L_s L_r}\right) \qquad (30)$$

$V_{dr}comp$ and $V_{qr}comp$ are nonlinear voltages that we have to compensate by control:

$$V_{dr}comp = w_r \sigma L_r L_{qr} \qquad (31)$$

$$V_{qr}comp = w_r \left(\sigma L_r L_{dr} + \frac{M}{L_s}\varphi_s\right) \qquad (32)$$

3. Control Strategies of DFIG

In conventional PID, the controller employments a power control loop to control active and reactive power. The reference value of active power is decided to agree to wind speed and the reference value of reactive power is set to zero. The pick-up of PID controllers is tuned based on the exchange work PID tuning application of MATLAB.

Fuzzy-based controllers can be outlined to function ideally in a wide extend of working focuses. By utilizing fuzzy logic, the framework can be controlled in a more solid way; externally, the tuning handle of the controller's parameters can be accomplished as it were by watching its behavior without knowing the detailed demonstration of the framework [23]. The common structure of a fuzzy controller has appeared in Fig.9. The FLC incorporates four fundamental intuitive instruments. The fuzzification unit decides inputs participation values to the fuzzy sets and the fuzzy inference system FIS assesses control rules to select

suitable ones. The two types of Fuzzy inference systems (FIS) are Mamdani and Takogi-Sugeno-Kong (TSK) strategies. Mamdani utilizes fuzzy sets to run the show ensuing. The reason for fuzzification is to bring inputs to values [19].The preeminent common fuzzy membership functions are triangular and Gaussian. The fuzzy control rules are based on the "if-then" method of reasoning sentences. The defuzzification unit computes the output of the rules concurring to the sort of fuzzy system into crisp values which are driven to the perfect plant control [24]. In Fig. 8 the input signals are error and its derivative (e and de/dt). The rotor voltage is utilized as output and the output control signal is the command's derivative (du/dt). These two signals are normalized through their particular scaling variables K_e and K_{de}. The output control signal is chosen by du/dt by the output scale calculated K_{du}, and after that encourages the creation of the command signal [9].

3.1 Fuzzy controller

In this technique, a fuzzy controller is utilized to control the whole rotor side converter. The controller is controlling the power, especially through the voltage vector output and each PI controller will be supplanted by a fuzzy controller. Fuzzy rules are for the most part developed based on data around control framework and operation standards. The fuzzy logic control is based on linguistic rules like:

Rule(i): IF $e = E$ and $de = dE$ THEN $du = dU$ (33)

Which fuzzy sets are selecting error as (E), the derivative of error (dE), and alter in control output incrementally (dU). Output (du) can be computed based on the two-dimensional stage plane as appeared in Table II. The sets have been characterized as NL: Negative Large, NM: Negative Medium, NS: Negative Small, ZR: Zero, PS: Positive Small, PM: Positive Medium, and PL: Positive Large. By considering 7 distinctive statuses for error and derivative of error, 49 control rules will be concluded. Gaussian function Fig.10 is received for membership functions (MFs) and Mamdani strategy for inference framework. The rules are organized to induce way better controller execution beneath diverse wind speed variety [5, 22].
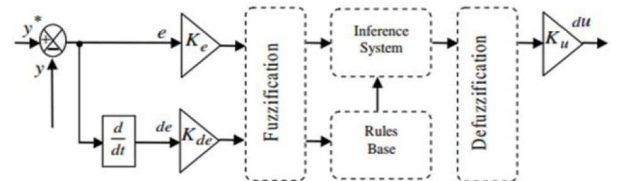
Fig. 9. Fuzzy Logic Structure
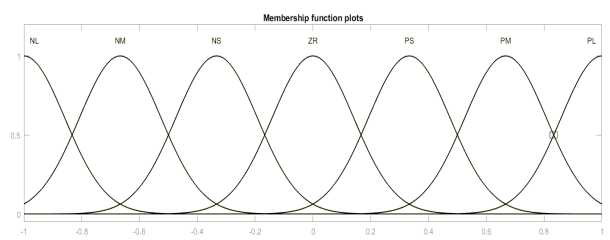
Fig.10. Gaussian Membership Function
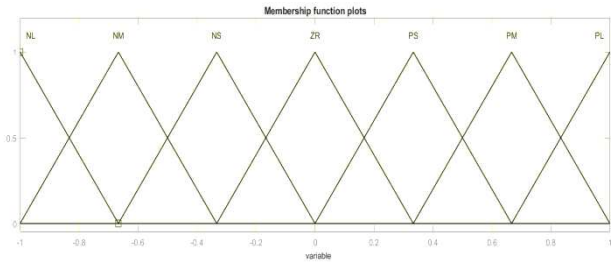
Fig.11. Triangular Memberships Function

Table II. Fuzzy rule base table

		Rule Base for *e, de, du*
		e
		NL	NM	NS	ZR	PS	PM	PL
De	NL	NL	NL	NL	NL	NM	NS	ZR
	NM	NL	NL	NL	NM	NS	ZR	PS
	NS	NL	NL	NM	NS	ZR	PS	PM
	ZR	NL	NM	NS	ZR	PS	PM	PL
	PS	NM	NS	ZR	PS	PM	PL	PL
	PM	NS	ZR	PS	PM	PL	PL	PL
	PL	ZR	PS	PM	PL	PL	PL	PL

3.2 Hybrid Fuzzy-PI Controller

In a hybrid Fuzzy-PI controller besides every fuzzy controller, a complementary PI controller is used. In PI controller, controlling parameters: proportional coefficient P=0.1 and Integral coefficient I=10 are manually set. These coefficients were obtained with the Ziegler-Nichols closed-loop tuning method [25]. The membership function for the first hybrid controller is Triangular represented in Fig. 11 and the second one is Gaussian. Controlling rules are similar to the fuzzy-based controller shown in TABEL II. In Table II Column 1 shows a derivative error and Row 2 shows an error. Output is the derivative of the controlling signal.

4. Simulation and Results

Simulation of PID, fuzzy, and hybrid fuzzy-PI controllers on the rotor side converter using MATLAB software has been done. RSC controls active and reactive powers at the stator side of DFIG. The turbine current in axis d (id) is modeled using the parameters of a 660 kW wind turbine. These parameters are listed in Table III. The goal is the comparison of PID, Fuzzy, and Hybrid Fuzzy-PI under a step change in wind speed. The rated wind speed in the mentioned wind turbine is 15 (m/s) and the wind cut-in and cut-out speed is 4 (m/s) and 25 (m/s) respectively. Due to changes in wind speed, reference output is active in the simulation, it is considered that wind speed was 9.9 (m/s) at

the beginning and changed to 24 (m/s) at 1 (sec) then slowing down to 7.5 (m/s) at 2 (s) Fig. 12.

TABLE III. INDUCTION GENERATOR PARAMETER

Rated Power	660 kW
Stator Voltage (line to line)	690 V
Stator Frequency	50 Hz
Rs	0.0064 p.u.
Xs	0.049 p.u.
Rr	0.006 p.u.
Xr	0.0589 p.u.
Pole Numbers	2
Cut-in Wind Speed	4 (m/s)
Rated Wind Speed	15 (m/s)
Cut-out Wind Speed	25 (m/s)
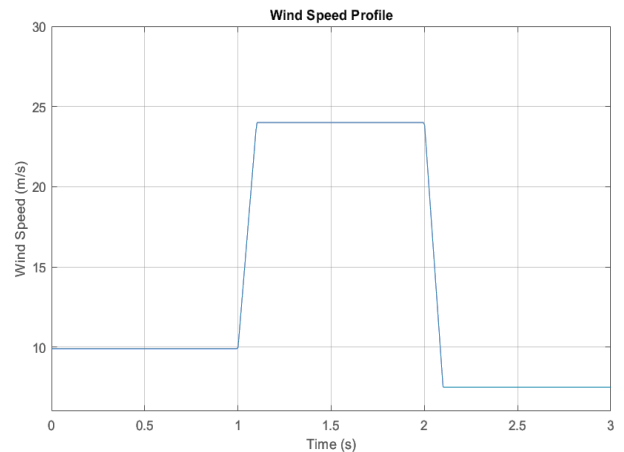
Fig 12. Wind Speed Profile
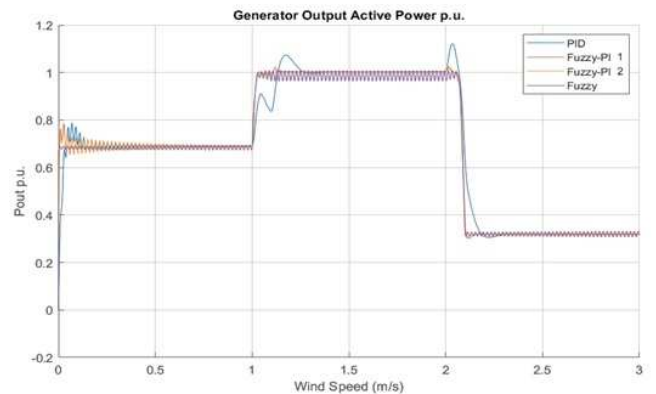
Fig. 13. Stator Side Output active Power
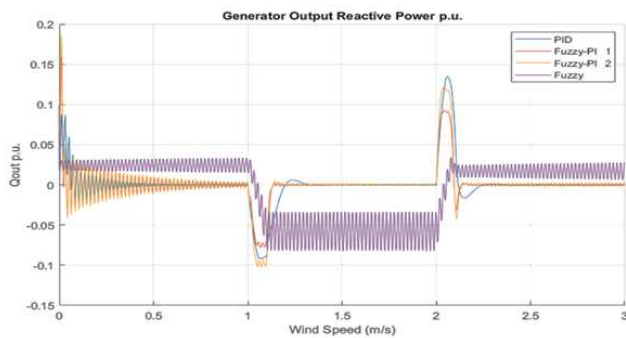
Fig. 14. Stator Side Output Reactive Power

Cp ratio maintained in optimum value. Reactive power controllers start to work in the unity power factor. Fig. 12 shows the wind speed available to the wind turbine and Fig. 13, Represented real power at the stator side of DFIG, using PID, Fuzzy, and Fuzzy-PI controllers. Actually, active power is negative, because it is getting out from the machine but we considered it as positive generating power. According to Fig. 12, the most overshoot and settling time belongs to the PID controller and the fuzzy controller could not match the proper settling time. However, Fuzzy-PI controllers show much better performance with insignificant differences. Fig. 14 depicts generated stator output reactive power. It is obvious that all controllers regulate output reactive power at 0 p.u. however; the fuzzy controller is not able to match it. This is resulted because of neglecting many system dynamics. According to Figure 13, in the active power of the Conventional PID controller generator, there are Ripples up to 0.25 seconds, as well as non-following of the Model within the minutes of 1 to 1.3 seconds and 16% overshoot. The fuzzy controller has ripples with a large volume of 0.03 at all times. Gaussian membership functions are used in hybrid fuzzy controller 2. This controller has ripples with the maximum amplitude of 4% from the start moment to 1 second and an overshoot of 7%. Triangular membership functions are used in hybrid fuzzy controller 1. This controller hasn't ripples and an overshoot of 7%. According to Figure 14, in the reactive power of the Conventional PID controller generator, there are Ripples up to 0.5 seconds, and the maximum amplitude of fluctuations is 0.14. The fuzzy controller has ripples with a large volume of 0.05 and error at all times. Gaussian membership functions are used in hybrid fuzzy controller 2. This controller has ripples with the maximum amplitude of 0.2 from the start moment to 1 second. Triangular membership functions are used in hybrid fuzzy controller 1. This controller hasn't ripples and the maximum amplitude of fluctuations is 0.08. A comparison of four controllers reveals that Hybrid PI Fuzzy with Triangular Membership

function experienced less overshoot, without error and ripple in output active and reactive power on the stator side.

5. Conclusion

This article examines the variable speed wind turbine generation system. Therefore, this system is prepared with a doubly-fed induction generator and two bidirectional converters in the rotor open circuit. DFIG could be a wound rotor induction generator that can be executed to bolster electrical power through both stators moreover rotor circuits. The stator feeds power straight to a unidirectional grid. The rotor circuit is associated with a bidirectional ac/dc/ac converter securing a common dc interface bus. This paper explores the hybrid fuzzy logic control of the DFIG wind turbine. All parameters and structures such as ponder framework, wind turbine, and control unit are depicted in points of interest. The performances have been tried on 660KW DFIG in a Matlab/Simulink software environment. Conventional PID, Fuzzy, and hybrid Fuzzy-PI controller with two diverse membership functions, Triangular and Gaussian membership function is displayed. Stator side output active and reactive power, mechanical and electromagnetic torque, and rotor speed for four strategies said compared. The comparison of simulations demonstrated that fuzzy-PI controller with Triangular membership function performs more successfully than other types. Fuzzy-PI with Triangular membership function appears marginally superior performance with hasn't ripples and an overshoot of 7% in the active power and hasn't ripples and the maximum amplitude of fluctuations is 0.08 in the reactive power.

References

[1] "Global Statistics Gwec," *Gwec*, 2022. [Online]. Available: http://gwec.net/global-figures/graphs/%0A.

[2] "Detailed statistics of Iran's power industry, power generation in 1390," in Detailed statistics of Iran's power industry, power generation in 1390, *Tavanir Specialist Company*, 2012.

[3] "Energy balance sheet of 1392," in Energy balance sheet of 1392, Tehran: Office of Planning for Electricity and Energy, Deputy of Electricity and Energy Affairs, *Ministry of Energy*, 2013.

[4] "Detailed statistics of Iran's power industry for strategic management in 1396," in Detailed statistics of Iran's power industry for strategic management in 1396, *Tavanir Specialist Company,* 2018.

[5] S. Demirbas, "Self-tuning fuzzy-PI-based current control algorithm for doubly fed induction generator," *IET Renew. Power Gener.*, vol. 11, no. 13, pp. 1714–1722, 2017.

[6] R. Pena, R. Cardenas, G. Asher, and Salvador Alepuz, "Overview of control systems for the operation of DFIGs in wind energy applications," *IECON Proc. Industrial Electron. Conf.*, vol. 60, no. 7, pp. 88–95, 2013.

[7] S. K. Raju and G. N. Pillai, "Design and Implementation of Type-2 Fuzzy Logic Controller for DFIG-Based Wind Energy Systems in Distribution Networks," Sustain. Energy, IEEE vol. 7, no. 1, pp. 345–353, 2016.

[8] E. Hosseini, N. Behzadfar,M. Hashemi, M. Moazzami, and M. Dehghani, "Control of pitch angle in wind turbine based on doubly fed induction generator using fuzzy logic method", *Journal of Renewable Energy and Environment (JREE)*, Vol. 9, No. 2, (2022), 1-7.

[9] A. Dida and D. Benattous, "Multilevel Converters using Fuzzy Logic Controller," *J. Control. Autom. Electr. Syst.*, vol. 26, no. 5, pp. 506–520, 2015.

[10] A.A. Chhipa, P. Chakrabarti, V. Bolshev, T. Chakrabarti, G. Samarin, A.N. Vasilyev, S. Ghosh, " Modeling and Control Strategy of Wind Energy Conversion System with Grid-Connected Doubly-Fed Induction Generator," *Energies,* vol. 15, 2022.

[11] S.M.H. Hosseini, A. Rezvani, "Modeling and Simulation to Optimize Direct Power Control of DFIG in Variable-Speed Pumped-Storage Power Plant Using Teaching–learning-Based OptimizationTechnique," *Soft Comput.* vol. *24*, pp. 16895–16915, 2020.

[12] A.A Chhipa, V. Kumar, S. Vyas, R.R. Joshi, "MPPT Optimisation Techniques and Power Electronics for Renewable Energy Systems: Wind and Solar Energy Systems. " *Int. J. Swarm Intell.* 2021, vol 1, no.1.

[13] H. Nian, Y. Xu, L. Chen and M. Zhu, "Modeling and Analysis of DC-Link Dynamics in DFIG System With an Indicator Function," in *IEEE Access*, vol. 7, pp. 125401-125412, 2019.

[14] S. Mishra, S. Shukla, N. Verma, and Ritu, "Comprehensive review on Maximum Power Point Tracking techniques: Wind Energy," *2015 Commun. Control Intell. Syst*., pp. 464–469, 2015.

[15] A. Acakpovi and E. Ben Hagan, "A Wind Turbine System Model using a Doubly-Fed Induction Generator (DFIG)," I*nt. J. Comput. Appl*., vol. 90, no. 15, pp. 6–11, 2014.

[16] DNV/Riso, Guidelines for Design of Wind Turbines, vol. 29, no. 2. 2002.

[17] E. Kulunk, Aerodynamics of Wind Turbines. 2011.

[18] T. Ackermann, Wind Power in Power Systems, vol. 140, no. February. 2005.

[19] J. Gambhir and T. Tilak, "Modeling and control of large wind farm based on DFIG using classical PI and Fuzzy Logic Controller (FLC)," *in International conference on Smart Technology for Smart Nation*, 2017, pp. 454–459.

[20] Vestas Wind Systems, "V47–660 kW with OptiTip and OptiSlip. [Online]," 2011. [Online]. Available: https://sti2d.ecolelamache.org/ressources/EE/premiere/ TP/serie 2/Vestas_V47.pdf.

[21] O. Rahat, "Enhancing Transient Stability in Limited Variable Speed Induction Generator (Optislip) Based Wind Turbine (Case study : Binalood Wind Farm)," *Eng. Technol. Appied Sci. Reseearch,* vol. 6, no. 6, pp. 1280–1287, 2016.

[22] F. Sastrowijoyo, K. Yim, and J. Choi, "Comparative study of PI and fuzzy controller for rotor side converter of DFIG," *in Conference Proceedings* - 2012 IEEE 7th International Power Electronics and Motion Control Conference - ECCE Asia, IPEMC 2012, 2012.

[23] A. Ashouri-Zadeh, M. Toulabi, S. Bahrami, and A. M. Ranjbar, "Modification of DFIG's Active Power Control Loop for Speed Control Enhancement and Inertial Frequency Response," *IEEE Trans. Sustain. Energy*, vol. 8, no. 4, pp. 1772–1782, 2017.

[24] M. Hilal, Y. Errami, M. Benchagra, and M. Maaroufi, "Fuzzy Power Control for Doubly," *J. Theor. Appl. Inf. Techno*l., vol. 43, no. 2, 2012.

[25] S. Muralidharan, T. Balasubramaniyam , K.S. Prethesh Kumar , C. Aswin, Performance analysis of controllers in BLDC motor, International Conference on Smart Engineering for Renewable Energy Technologies, Tamil Nadu, India , march 2023.